Journal Pre-proof

Twin crystal structured Al-10 wt.% Mg alloy over broad velocity conditions achieved by high thermal gradient directional solidification

Luyan Yang, Shuangming Li, Kai Fan, Yang Li, Yanhui Chen, Wei Li, Deli Kong, Pengfei Cao, Haibo Long, Ang Li

PII: S1005-0302(20)30805-7

DOI: https://doi.org/10.1016/j.jmst.2020.07.032

Reference: JMST 2547

To appear in: *Journal of Materials Science & Technology*

Received Date: 29 May 2020

Revised Date: 15 July 2020

Accepted Date: 27 July 2020

Please cite this article as: { doi: https://doi.org/

Research Article

Twin crystal structured Al-10 wt.% Mg alloy over broad velocity conditions achieved by high thermal gradient directional solidification

Luyan Yang [a, b, c], Shuangming Li [b*], Kai Fan [b], Yang Li [b], Yanhui Chen [a*], Wei Li [a], Deli Kong [a, c], Pengfei Cao [c], Haibo Long [a], Ang Li [a]

[a] *Institute of Microstructure and Properties of Advanced Materials, Faculty of Materials and Manufacturing, Beijing University of Technology, Beijing 100124, China*

[b] *State Key Laboratory of Solidification Processing, Northwestern Polytechnical University, Xi'an 710072, China*

[c] *Ernst Ruska-Centre for Microscopy and Spectroscopy with Electrons, Forschungszentrum Jülich, 52428 Jülich, Germany*

Corresponding authors: Shuangming Li, Prof., Ph.D., Tel.: +86 02988493264, Fax: +86 02988493264, E-mail: lsm@nwpu.edu.cn; Yanhui Chen, Ph.D., Tel.: +86 01067396521, Fax: +86 010 67396521, E-mail: yhchen@bjut.edu.cn.

[Received 29 May 2020; Received in revised form 15 July 2020; Accepted 27 July 2020]

Abstract

Twin crystal structured Al-10 wt.% Mg alloys that were grown over a broad solidification velocity range were prepared and studied for the first time. The high thermal gradient (G) and growth velocity (V) of directional solidification resulted in the dominant solidification of twins: the twinned dendrite trunks at constant high Vs curved in the G direction with large angles in 7 mm diameter crucibles and invaded regular columnar grains because of a distinct kinetics growth advantage. Transitive deceleration experiments were designed to produce twin crystals that evolved with lower values of V (100, 10, and 0.5 μm/s) and had a structural coarsening trend. Twin cell growth in the absence of arms occurred at a growth velocity of 10 μm/s. A coherency loss was observed at a growth velocity of 0.5 μm/s with straight coherent twin boundaries turning into curved incoherent boundaries. Linear theoretical analyses were performed to understand the structural evolution of the twins. These results demonstrate the possibility of producing dense and controlled twin crystals in the Al-Mg system under most industrial production conditions; thus, this approach can be a new

structural choice for designing Al-Mg-based alloys that have widespread commercial applications.

***Keywords*:** Directional solidification; Aluminum alloy; Microstructural evolution; Feathery crystals; Twinned dendrites;

1. Introduction

Dendritic crystals are the main structural constituents of solidified metallic alloys and primarily determine their final properties and qualities during solidification and subsequent forming processes [1-4]. In particular, feathery twin crystals composed of special <110> twinned dendrites in Al alloys, have received considerable research attention since they were first observed in industrial casting practice [5-9]. On the basis of a series of electron backscatter diffraction (EBSD) investigations, Henry et al. [7, 10] identified that, in contrast to the usual <100> regular columnar dendrites in metallic alloys, there was a straight {111} coherent twin boundary in the center of the <110> twinned dendrite trunk. The secondary arms of the twinned dendrites grew in the <110> or <100> direction, and the arm impingement of neighboring twinned dendrites usually created wavy incoherent twin boundaries.

Feathery twin crystals, (i.e., twinned dendrites) were observed to preferentially occur in direct-chill or semi-continuous casting processes, and the specific formation conditions are summarized as follows: a thermal gradient (G) of ~ 100 K/cm, a high growth velocity (V) above 1 mm/s, and relatively strong melt convection [7, 11, 12]. Meanwhile, Kurtuldu et al. [13, 14] demonstrated that adding a minor amount of Cr to solidified Al-20 wt.% Zn alloys induced a large number of twin and near-twin relationships between neighboring grains. Nearest neighboring grains exhibited a fivefold rotation symmetry multi-twinning relationship around a nearly common direction, specifically, the <110> direction. Twin nucleation was proposed to occur on the basis of the formation of quasicrystal pre-nuclei in

the liquid phase. Concerning the growth stability of twinned dendrites, Salgado-Ordorica et al. [15] studied the evolution of structures that resolidified from prepared Al–23 wt.% Zn twin seeds at velocities of 66 and 330 μm/s. In this case, the twin morphology did not remain stable, and only regular dendrites grew epitaxially from the seeds. However, in a different directional solidification experiment, the twin structures in an Al-4.5 wt.% Cu alloy continued at a low velocity of 1 μm/s [16]. There are still some unclear aspects of twin growth behavior that require additional investigation.

It is known that solute elements play an essential role in the formation of twinned dendrites in Al alloys [7, 17]. Mg is a typical hcp element and tends to modify the local atomic arrangement and promotes twin formation in fcc structures. Additionally, Mg in Al alloys always causes a change in the dendrite growth directions from <100> to <110> at relatively high solute compositions [17, 18]. Thus, Mg undoubtedly favors twin formation in Al alloys. However, until now, there have been few reports on twin structures in Al-Mg alloys. Also, there have been no systematic studies performed on twinned dendrite growth in Al-Mg alloys with directional solidification, which is a technique that is beneficial for understanding the fundamentals of solidified microstructures via independent control of G and V [19-22]. Also, given the vital application of Al-Mg-based industrial alloys [23-26], an in-depth study of the diverse microstructures in Al-Mg alloys, including the twin crystal structures, is needed.

In this work, feathery twin crystals in an Al-10 wt.% Mg alloy were successfully produced using the Bridgman solidification technique within a broad V range. We systematically investigated the microstructures and growth characteristics of the twin crystals in the Al-10 wt.% Mg alloy. Also, the twin growth stability and corresponding microstructural development were investigated using a V transition deceleration method. On the basis of these experimental results, theoretical analyses were performed to elucidate the twin

evolution.

2. Experimental methods

An ingot comprising Al-10 wt.% Mg was used in the experiments and was prepared via the vacuum induction melting method using high-purity Al (99.999 wt.%) and Mg (99.999 wt.%). The amount of trace elements in the alloy ingot was analyzed using inductively coupled plasma optical emission spectrometry (ICP-OES, Agilent 725) and found to be: Si (0.021 wt.%), Sn (0.015 wt.%), Fe (0.008 wt.%), Mn (0.004 wt.%), and other elements (<0.001 wt.%).

Directional solidification samples with a diameter of 7 mm and a length of 180 mm were machined from the as-cast ingot and placed into a high-purity alumina crucible. An improved Bridgman solidification apparatus with liquid metal cooling was used, which is described in detail elsewhere [9]. During the directional solidification experiments, the alloy samples were first heated to ~750 °C and then maintained at this temperature for ~30 min, then pulled downwards into the liquid metal bath at various values of V. For directional solidification at a constant V, the melted samples were pulled down at 500, 1000, 1500, 2000, and 3000 μm/s over a distance of 80 mm, and then quenched. For directional solidification under the transitive deceleration method, the melted samples were first pulled down at 3000 μm/s over a distance of 80 mm and then pulled with a lower V of 100, 10, or 0.5 μm/s over a distance of 100 mm. It is known that a high thermal gradient plays an important role in promoting the formation of twinned dendrites in Al alloys [7, 9]. The thermal gradient in the liquid ahead of the solid-liquid (S/L) interface was measured in directional solidification experiments, and the average value was ~269K/cm, which greatly promoted the dominant solidification of twins.

The as-solidified sample sections were polished mechanically and etched with dilute Keller's reagent (1 mL HF, 3 mL HNO_3, and 46 mL H_2O) for metallographic observations in

an Olympus TG-3 optical microscope. For EBSD characterization, selected microstructure sections were first mirror-polished and then etched electrochemically to eliminate the deformed surface layers. EBSD investigations were performed on a Tescan Mira 3 FEG scanning electron microscope equipped with an Oxford Instruments HKL Nordlys Max EBSD system. EBSD data collection and post-analysis were completed using the HKL Channel 5 software package.

3. Results and discussion

3.1 Twinned dendrites in Al-10 wt.% Mg alloy at constant growth velocities

3.1.1 Microstructure and growth characteristics

Fig. 1 shows typical microstructures in the directionally solidified Al-10 wt.% Mg alloys at constant V values of 500, 1000, 1500, 2000, and 3000 μm/s. The twinned dendrites and regular columnar dendrites are indicated with "T" and "R", respectively. The direction of the thermal gradient (G) is indicated with an arrow. These well-developed dendritic structures achieved steady-state solidification under their respective conditions. In general, once nucleation occurred, a feathery twin crystal in Al alloys would develop from the nucleation point with a characteristic fan shape [7, 11]. The twinned dendrite microstructure is composed of a sequence of alternating twinned and untwinned lamellae that can appear disoriented with G direction progressively. Similarly, in this work, we observed that the growth direction of twinned dendrites in Al-Mg alloys mostly presented several angles with that of G during directional solidification.

Fig. 2 shows the overall longitudinal morphology for solidification at 500, 1500, and 3000 μm/s. Feathery twin crystals nucleated and multiplied rapidly as solidification proceeded, and the twinned dendrites dominated the final microstructure with a significant growth kinetic advantage over the regular columnar dendrites. Multiple twinned dendrite grains were present in each solidification condition and in Fig. 2, these are marked as T*i*,

where i=1, 2, 3, and 4. In the directional solidification of this work, the higher thermal gradient and growth velocities, which correspond to higher cooling rates ($G \cdot V$), indeed improved the possibility of the twin nucleation and thus resulted in solidified structures that contained several twin grains.

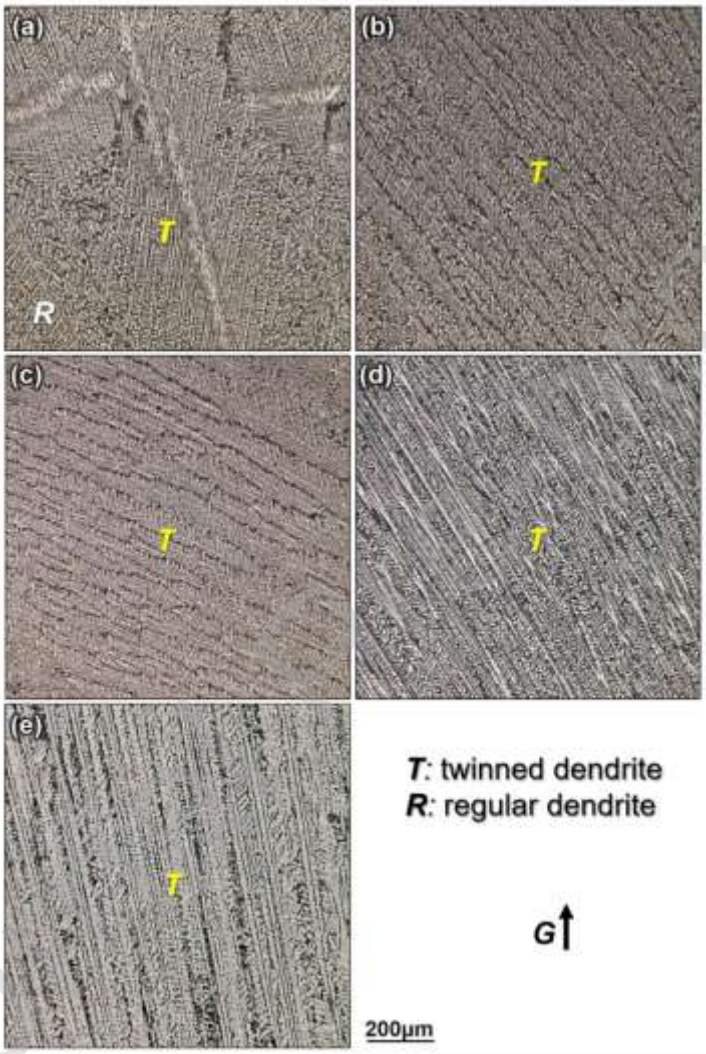

Fig. 1. Typical twinned dendrite microstructures in directionally solidified Al-10 wt.% Mg alloys at constant growth velocities of (a) 500 μm/s, (b) 1000 μm/s, (c) 1500 μm/s, (d) 2000 μm/s, and (e) 3000 μm/s. The arrow indicates the direction of the thermal gradient *G*. Twinned dendrites and regular columnar dendrites are indicated with "T" and "R", respectively.

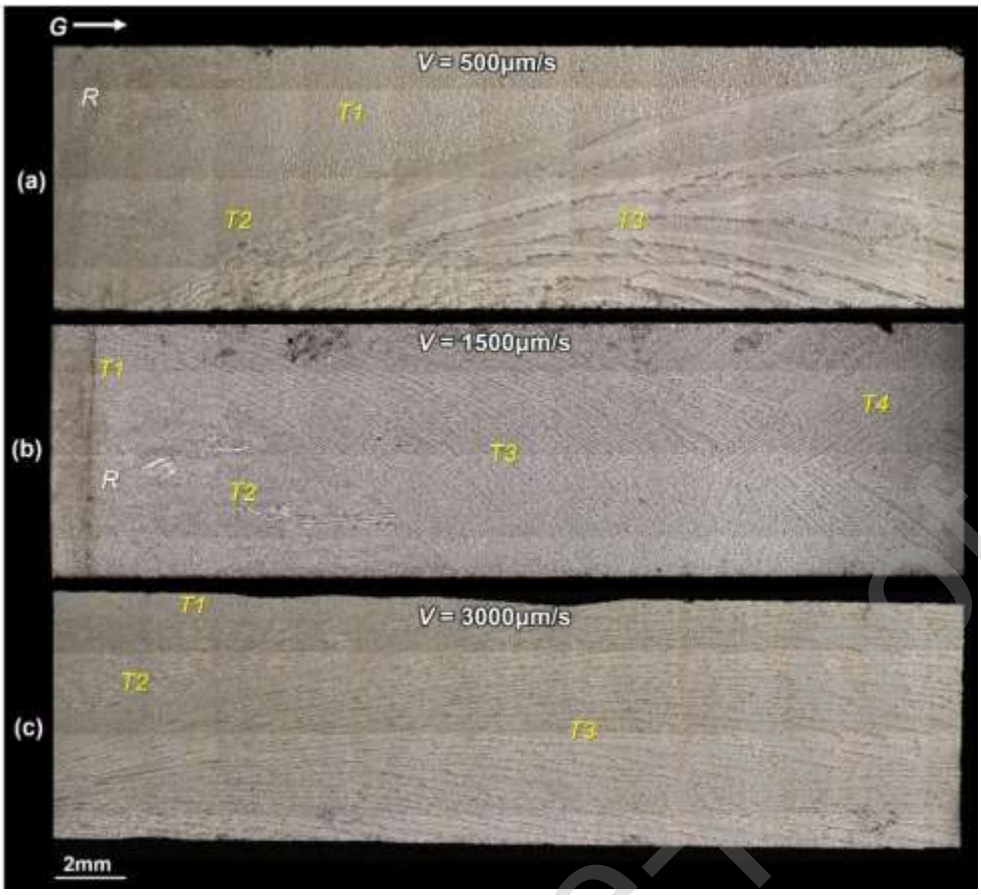

Fig. 2. Overall view of the longitudinal microstructure in the directionally solidified Al-10 wt.% Mg alloys at constant velocities of (a) 500 μm/s, (b) 1500 μm/s, and (c) 3000 μm/s. Twinned dendrite grains are marked with T*i*, where *i*=1,2,3, and 4.

It is noted that twinned dendrite growth in the Al-Mg system was fairly active even under the constrained condition of directional solidification. In contrast to the very straight trunks of the twinned dendrites in the Al-Cu alloys [9], the twinned trunks in the Al-Mg alloys studied herein were curved along the *G* direction with relatively large angles. In Fig. 2(a) and (b), most of the twinned trunks that solidified at 500 and 1500 μm/s bent continuously in the *G* direction until they collided with the crucible wall and then developed distinct fan-shaped features. It was only when the solidification reached a growth velocity of 3000 μm/s that the twinned dendrite growth could be controlled, and in this case, the trunks became almost parallel to the *G* direction (Fig. 1(e) and Fig. 2(c)).

It is known that when the growth velocity is increased, the growth direction of regular columnar dendrites tends to change from the *G* direction to a preferred crystalline orientation

([100] for fcc structure), which thus induces a relatively large growth deviation [27, 28]. However, twin solidification showed a different trend and the growth direction of the twinned trunks at 3000 μm/s appeared to be more parallel to the *G* direction, whereas large growth deviation occurred for twinned dendrites at 500, 1000, 1500 and 2000 μm/s (Fig. 1 and Fig. 2). These phenomena should be caused by the special nucleation and growth processes of <110> twinned dendrites, which is different from the <100> regular columnar dendrites. As mentioned above, the nucleation of twinned dendrites was closely related to the formation of quasicrystal pre-nuclei in the liquid, and subsequent twinned growth can be seen as heteroepitaxial growth on an icosahedral template [13]. Therefore, the growth direction of twinned dendrites was strongly influenced by the crystalline orientation of the formed quasicrystal pre-nuclei. Meanwhile, the twinned dendrites have a special kind of plate-like growth type [29], and their efficient lateral twin propagation perpendicular to the twin plane at a high velocity helps the dominated twin solidification over regular grains, accompanying the twin trunks almost parallel to the *G* direction.

Moreover, in the Bridgman solidification experiments in this work, it should be noted that although some dendrite primary trunks presented a relatively large angle with *G* (especially in Fig. 1(c) and Fig. 2(b)), no columnar to equiaxed dendrite transformation was observed during steady solidification. Also, most equiaxed grains only formed during quenching as will be discussed below. This suggests that the solidification processes herein (up to 3000 μm/s) were within the scope of directional solidification.

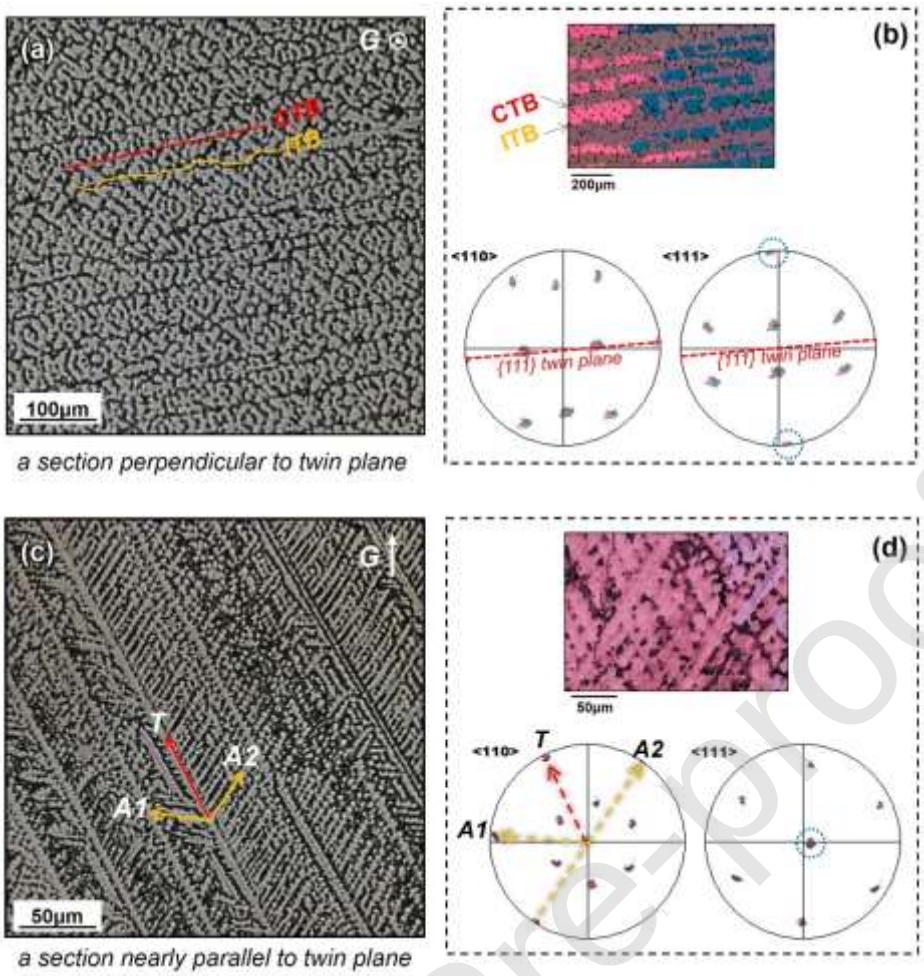

Fig. 3. (a) Twinned dendrite microstructures that solidified at 3000 μm/s in a section perpendicular to the {111} twin plane, and (b) corresponding EBSD map and <110> and <111> pole figures. (c) Twinned dendrite microstructures that solidified at 3000 μm/s in a section nearly parallel to the {111} twin plane, and (b) corresponding EBSD map and pole figures. The red lines in the pole figures indicate the {111} twin planes. The common <111> directions are circled in the pole figures.

The crystallographic orientation of Al-10 wt.% Mg twinned dendrites that solidified at 3000 μm/s was investigated on two sections of the sample in detail using EBSD. Fig. 3(a) and (b) show the metallographic structure in a section that is perpendicular to the {111} twin plane, the corresponding EBSD map, and the <110> and <111> pole figures (PFs). Clearly, the twinned dendrite grains were composed of a series of parallel twin lamellae that were alternately separated by coherent and incoherent twin boundaries (CTBs and ITBs, respectively). In the <110> PF shown in Fig. 3(b), a total of nine clusters of poles (<110> directions) can be distinguished. Among them, three common <110> directions were located along the {111} twin plane (indicated by a red line). This observation reveals that the two

pairs of twin domains shared one common {111} twin plane and three common <110> dendrite growth directions. The other six uncommon <110> directions were symmetrically distributed with respect to the common {111} twin plane, which indicates an exact twin relationship. In the <111> PF shown in Fig. 3(b), the circled cluster is a common <111> direction, which corresponds to the normal of the {111} twin plane.

Fig. 3(c) and (d) show the microstructure in a section that is nearly parallel to the {111} twin plane and the corresponding EBSD results. Fig. 3(c) clearly shows the dendritic structures that are contained in the {111} twin plane. In the <111> PF in Fig. 3(d), the common <111> direction was almost at the center zone (indicated by the circle), and this confirms that the observed section corresponds to the {111} plane. In the <110> PF shown in Fig. 3(d), there are three common <110> directions (T', A1', and A2') located near the edge of the <110> PF, and these are parallel to the dendrite directions, T, A1, and A2, as shown in Fig. 3(c). This reveals a <110> growth direction for both the dendrite trunk and side arms of the twinned dendrites.

As observed from Fig. 2, directional solidification induced nucleation and growth of several twin crystal grains in each experiment. Fig. 4(a-b) shows EBSD results near the nucleation region of the twinned dendrites in the Al-10 wt.% Mg alloy that solidified at 1500 μm/s. In Fig. 4(a), three twin grains initially nucleated and converged. Fig. 4(b) shows the assemblage of <110> PFs for grains T1, T2 and T3. Clearly, the nucleation processes of these three grains did not affect each other, and independently formed twins, each with a respective common {111} twin plane (indicated by red arcs in PF). For the subsequent twin growth process, Fig. 4(c) and (d) show an EBSD map and the corresponding <110> PF of two twinned dendrite grains that cross-grew during steady-state solidification at 1500 μm/s. As seen, these two twin grains (T4 and T5) exhibited complex overlapping dendritic structures and maintained their growth mode of twin lamellae during their cross-growth.

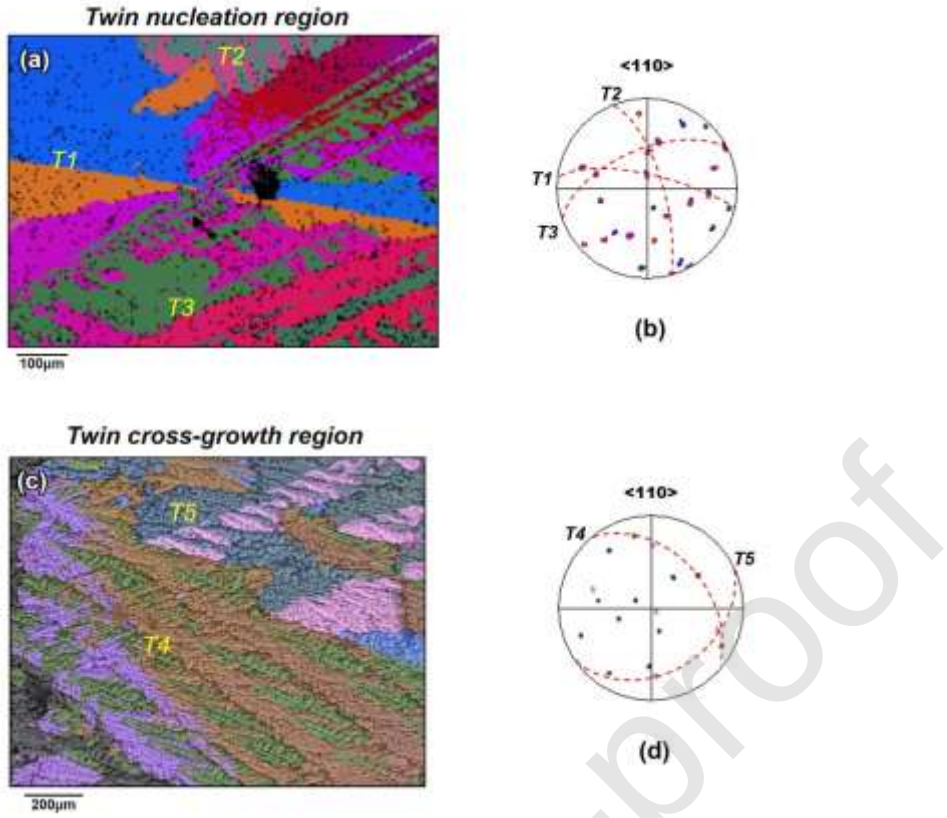

Fig. 4. (a-b) SEM and EBSD maps near the nucleation region of the twinned dendrites in the Al-10 wt.% Mg alloy solidified at 1500 μm/s. (c) Corresponding <110> and <111> pole figures of grains T1, T2, and T3 in (a-b). (d) The assemblage of three <110> pole figures of grains T1, T2, and T3. (e-f) EBSD map of twin grains T4 and T5 cross-growth during steady-state solidification at 1500 μm/s, and the corresponding pole figures. The red arcs mark the {111} twin plane of each twin grain. The blue circles indicate the nearly common <110> axes with a misorientation spread of 9-10°.

3.1.2 Quenched morphology of Al-10 wt.% Mg twinned dendrites

Fig. 5(a) and (b) show the quenched microstructure evolution of twinned dendrites that solidified at 3000 μm/s and a magnified view near the solid-liquid (S/L) interface. After quenching, equiaxed grains impeded growth of the tapering twinned dendrite trunks. Interestingly, as indicated by the yellow dotted trace lines in Fig. 5(a), the fine twinned dendrite trunks also began to bend further into the mushy zone. The main reasons for this phenomenon could be the instant increase in the growth velocity during quenching and the natural convection that occurs ahead of the S/L interface. It is known that dendritic trunks and side arms usually exhibit pronounced growth and bend toward the incoming direction of the melt flow [10, 12, 30]. The bending behavior of the quenched twinned dendrites also induced

the evolution of the orientation. Fig. 5(d) and (e) show the corresponding EBSD map and PFs of twinned dendrites in the mushy zone. It is noted that the spread of all of the clusters in the PFs expanded simultaneously, which implies a certain degree of orientation adjustment during twinned dendrite growth. Accordingly, the misorientation evolution along the direction indicated by the arrow in Fig. 5(d) was measured and is shown in Fig. 5(f). The misorientation profile relative to the starting point reveals the existence of an orientation adjustment of ~9° during the quenching of the twinned dendrites.

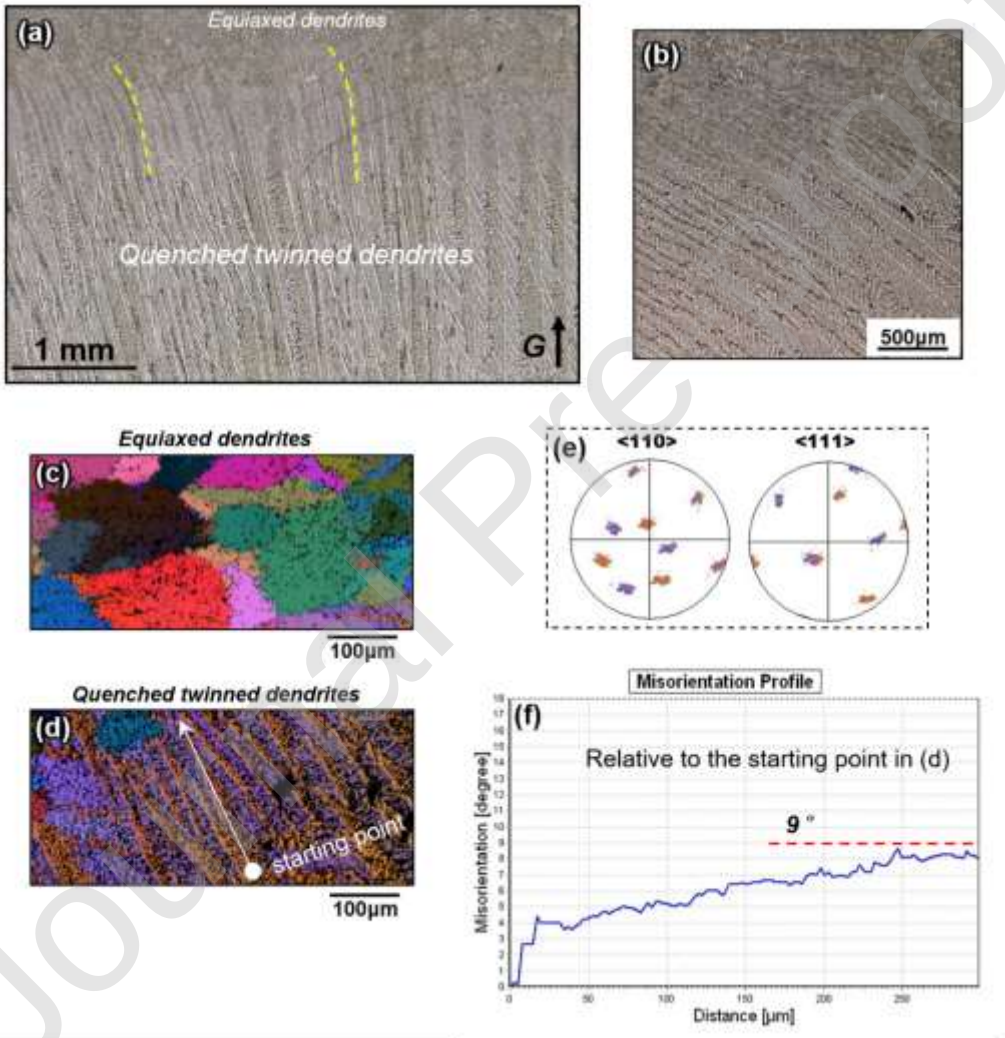

Fig. 5. (a) Quenched microstructure of Al-10 wt.% Mg alloy directionally solidified at 3000 μm/s and (b) a magnified view. EBSD maps of (c) equiaxed dendrites and (d) twinned dendrites formed during quenching. (e) Corresponding <110> and <111> pole figures of twinned dendrites shown in (d). (f) Misorientation profile along the white arrow line relative to the starting point in (d).

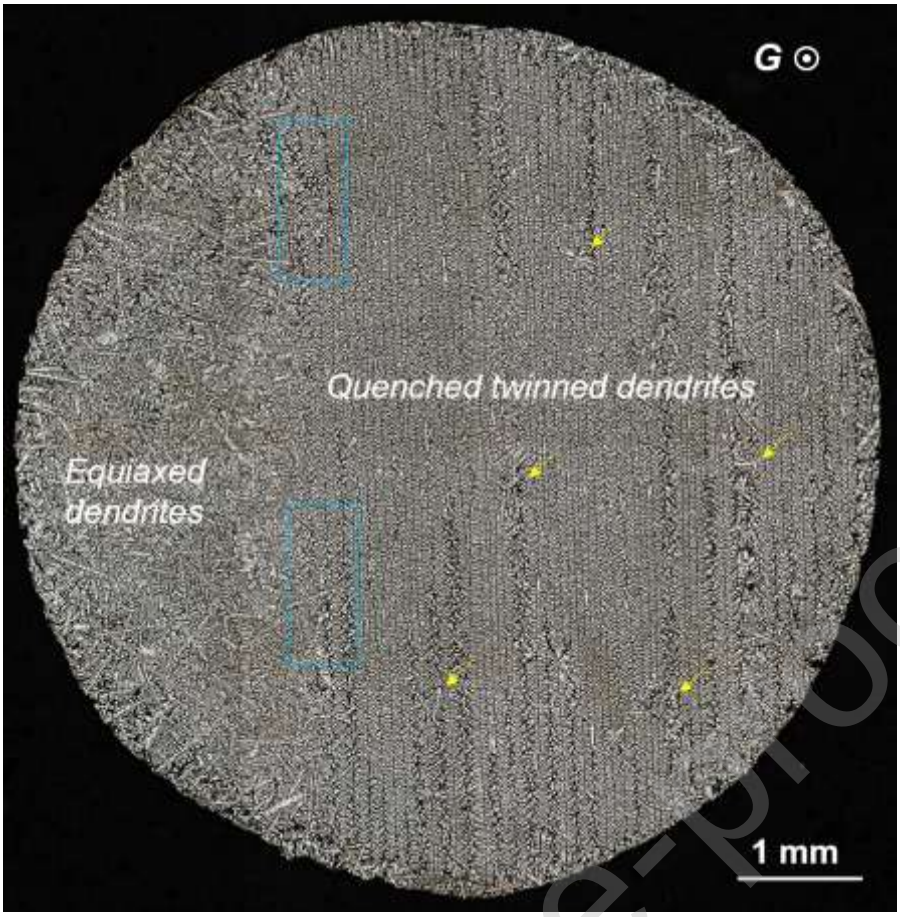

Fig. 6. Transverse view of the quenched microstructure of Al-10 wt.% Mg alloy directionally solidified at 3000 μm/s.

During quenching, the termination of twinned dendrite growth was a gradual process. Fig. 6 shows the transverse microstructure in the mushy zone. The lamellar feature of twinned dendrite growth is distinctly different from the features of equiaxed dendrites, which were disordered. As indicated by yellow arrows, small equiaxed dendrites frequently nucleated and grew in the narrow liquid phase between adjacent twin lamellae, and this caused the lamella of continuous twin trunks to break. As indicated by blue rectangles, the formation of equiaxed dendrites destroyed twin lamellae at two positions in the middle region. These findings suggest that the growth of twinned dendrites during quenching was not entirely stopped by the equiaxed grains that formed in the liquid phase further ahead, as has usually been supposed. With the above mechanism, equiaxed grains that formed within the liquid phase between the twin lamellae also gradually stopped the growth of the twinned

dendrites in the mushy zone. It seems that during the free solidification after quenching, the twinned dendrites had no obvious advantage in terms of growth kinetics over equiaxed dendrites, and the low velocity provided an equal opportunity for their growth.

3.2 Twin crystal structured Al-10 wt.% Mg alloy under decreasing growth velocity conditions

Transitive deceleration experiments were designed to achieve twin crystals in Al-Mg alloys that evolved at lower values of V (100, 10, and 0.5 μm/s) based on twinned dendrites growing at constant 3000 μm/s. By introducing a decrease in V during directional solidification, the growth stability and structural evolution of twin crystals with various lower values of V were also investigated.

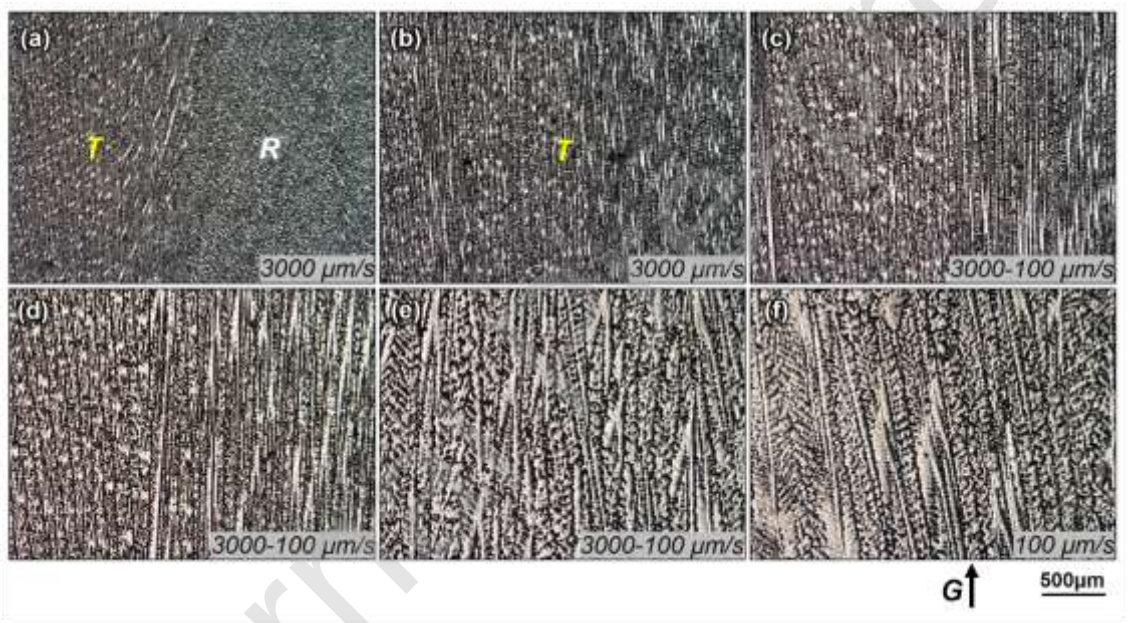

Fig. 7. Evolution of the longitudinal microstructure in the directionally solidified Al-10 wt.% Mg alloy with a growth velocity that was decreased from 3000 μm/s to 100 μm/s.

Fig. 7 displays the evolution of longitudinal microstructure with the value of V changing from 3000 μm/s to 100 μm/s. From Fig. 7(a) to (b), it is seen that twinned dendrites dominated the entire volume of the microstructure that was solidified at 3000 μm/s, relying on their growth advantage over the regular columnar dendrites. Fig. 7(c-e) correspond to the transition process after V was decreased to 100 μm/s, and it shows an apparent structural coarsening trend. Fig. 7(f) displays the steady-state microstructure at 100 μm/s. In comparing

Fig. 7(f) with (b), it is seen that the final twin microstructures at 100 μm/s presented coarser twinned trunks and side arms than those at 3000 μm/s. Also, after the decrease from 3000 μm/s, the twinned dendrites maintained their growth direction at 100 μm/s, which is almost identical to the *G* direction. This is attributed to the history-dependent growth of the transient deceleration method [31]. A similar trend was previously reported for regular columnar dendrites, twinned dendrites and eutectic structures during directional solidification of Al alloys [16, 31, 32].

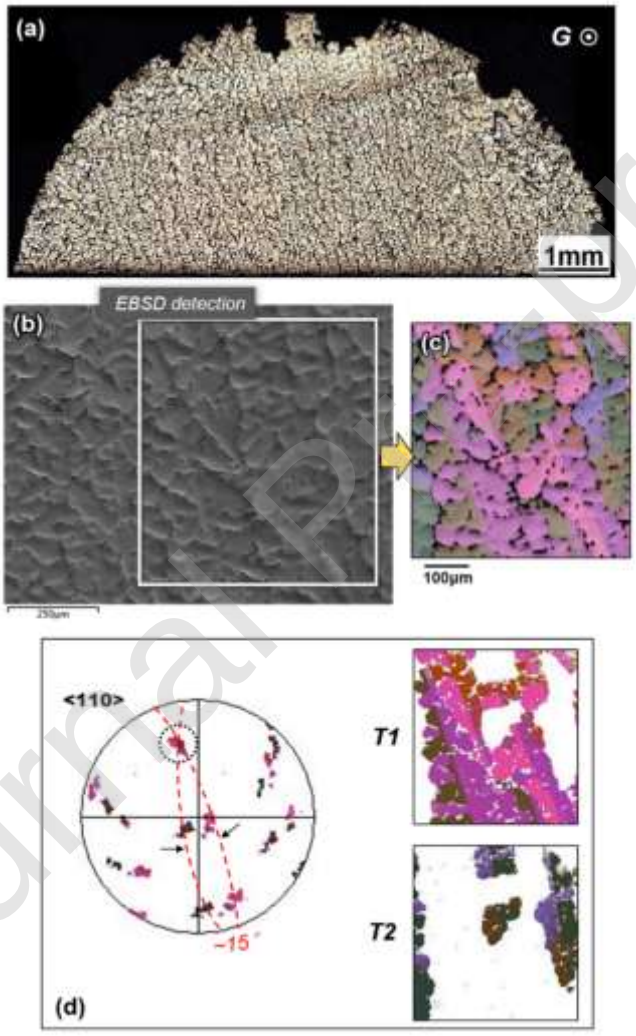

Fig. 8. (a) The steady-state transverse microstructure of the Al-10 wt.% Mg alloy that was solidified at 100 μm/s, which was decreased from 3000 μm/s. (b-c) SEM and EBSD maps of two coexisting twinned dendrite grains T1 and T2 shown in (a). (d) The orientation relationship between grains T1 and T2, including the <110> pole figure. The red arcs indicate the {111} twin planes.

In the transverse structures at 100 μm/s, which was from 3000 μm/s (Fig. 8(a)), two sets

of parallel twinned dendrites were present, and each set can be defined as one twin grain. SEM and EBSD maps of these two coexisting grains are displayed in Fig. 8(b) and (c); their orientation relationship was analyzed and is shown in Fig. 8(d). Clearly, in the <110> pole figure, grains T1 and T2 shared the same <110> common direction, which served as the intersection of two {111} twin planes (red arcs). These two twin crystals were rotated approximately 15° around this common <110> direction. This kind of crystallographic orientation can be attributed to the structural adjustment after solidification deceleration. Also, despite the small angle (~15°) between the two {111} twin planes (Fig. 8(d)), the above observation corresponds closely to a five-fold symmetric multi-twinning relationship around a nearly common <110> direction, as recently reported for an Al–Zn–Cr alloy, which suggested the critical role of icosahedron quasicrystals in the nucleation of twinned dendrites [13, 33].

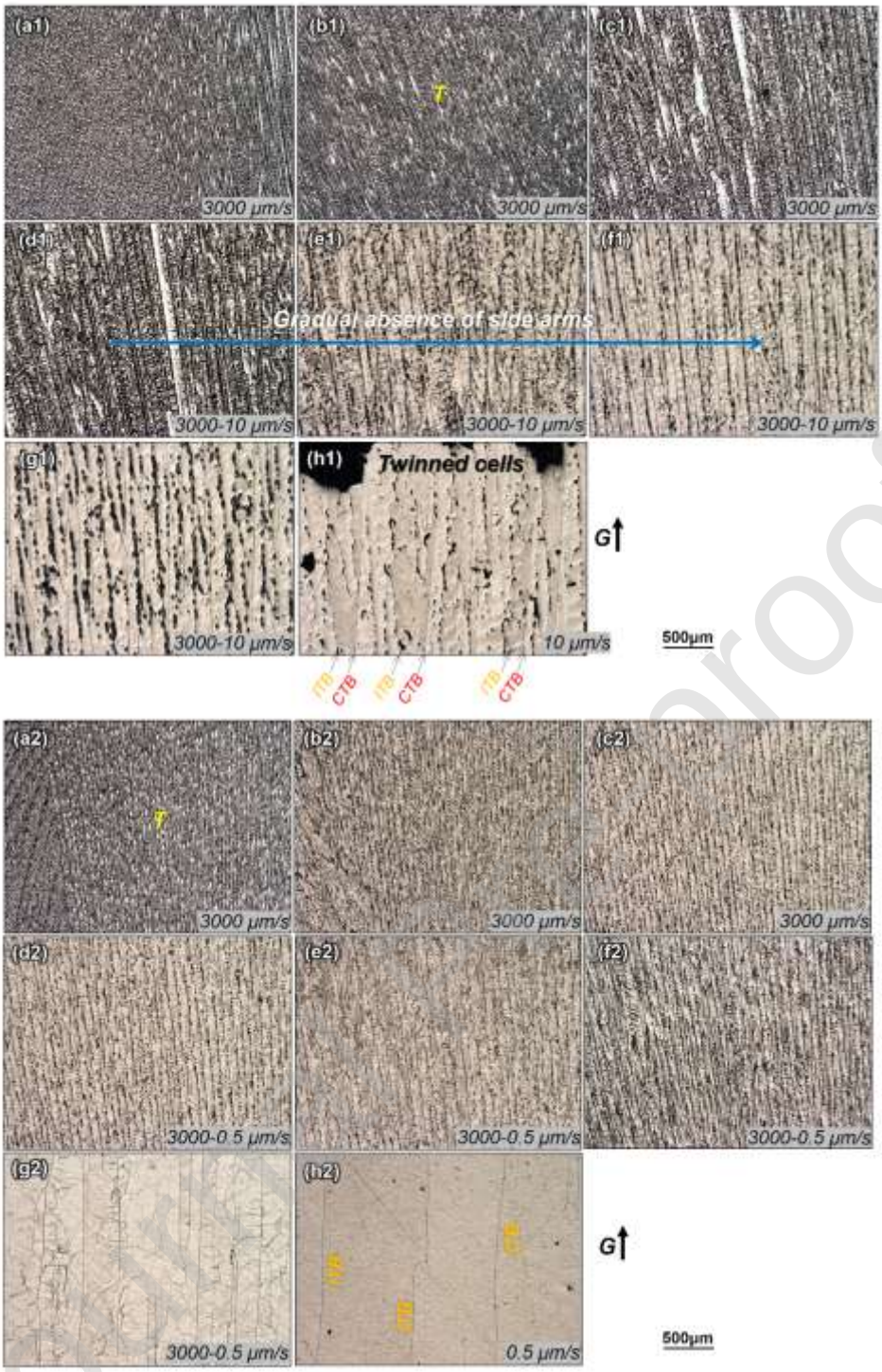

Fig. 9. Evolution of the longitudinal microstructure of the directionally solidified Al-10 wt.% Mg alloy with the growth velocity that wad decreased from 3000 μm/s to 10 μm/s (a1-h1), and decreased from 3000 μm/s to 0.5 μm/s (a2-h2). The blue arrow in (d1-f1) indicates the gradual absence of side arms and the transformation from twinned dendrites to twinned cells (h1).

Fig. 9 (a1-h1) shows the evolution of the microstructure with respect to changing V from 3000 μm/s to 10 μm/s. From Fig. 9(d1) to (f1), it is seen that with decreasing V, the side arms of the twinned dendrites faded away, and in the final solidification at 10 μm/s (Fig. 9(h1)),

there are only some small droplets that appeared within the twin domains and twin boundaries. This kind of growth morphology falls in the scope of cellular solidification and can be called a twinned cell in the Al-Mg system, following the nomenclature of the "twinned dendrite" term. It should be noted that the structural feature of alternating CTB and ITB of twinned dendrites was still retained in the twinned cells (as marked in Fig. 9(h1)).

When V was decreased to 0.5 μm/s, as seen in Fig. 9 (a2-h2), the twin microstructure underwent additional coarsening and finally displayed distinct and sparse boundary lines. In contrast, as seen in Fig. 9(g2) and (h2), the rather low V of 0.5 μm/s seemed to impair twin solidification, and a loss of coherency of the central twin boundaries occurred, with a transformation from straight (CTBs) to slightly curved (ITBs). In this case, we should not discuss twinned dendrite or cellular growth. The microstructure seen in Fig. 9(h2) is, in fact, the independent growth of twinned and untwinned domains at 0.5 μm/s, and not of a specific growth morphology. A similar coherency loss of twin boundaries was observed in a regrowth process based on twinned dendrite seeds [15]. The results showed that regular dendrites regrew from the seeds, and the original CTB in the seeds could not be maintained and formed a flexuous boundary with an incoherent twinning relationship instead.

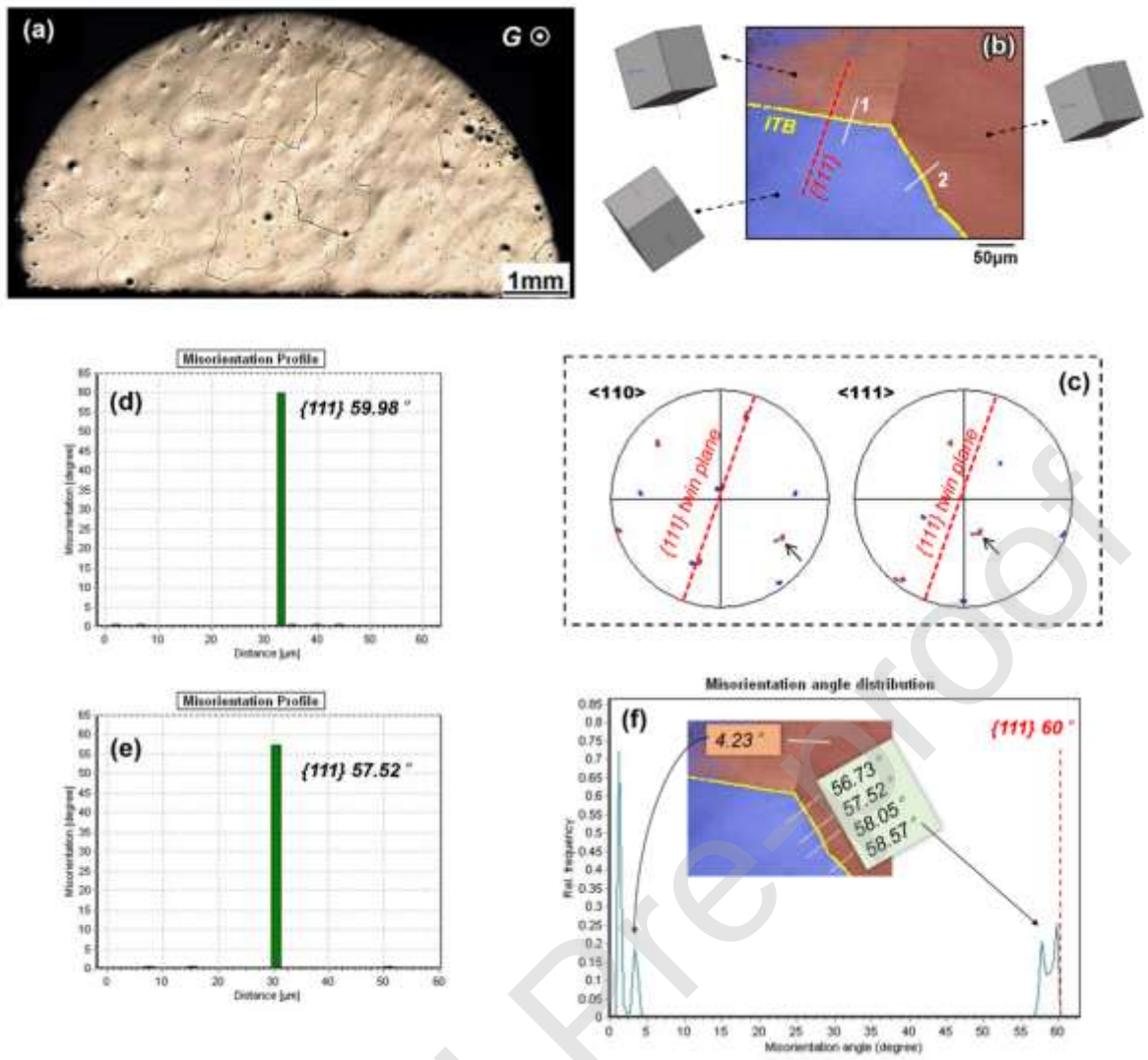

Fig. 10. (a) Steady-state transverse microstructure of Al-10 wt.% Mg alloy at 0.5 μm/s, which was decreased from 3000 μm/s. (b) Typical EBSD map containing an incoherent twin boundary (yellow line) created by the independent growth of twin domains. Three-dimensional crystal orientations acquired from different regions are provided. (c) Corresponding pole figures of (b). The red lines in (b) and (c) indicate the {111} twin planes. (d-e) Misorientation profiles measured along the white dotted lines 1 and 2 crossing boundaries shown in (b). (f) Overall misorientation angle distribution in (b). The inset shows several misorientation angles measured crossing different boundaries.

The transverse morphology for solidification at 0.5 μm/s further confirmed the coherency loss. In Fig. 10(a), the lamellar feature of the twinned dendrite growth disappeared, and the microstructure showed boundaries that only had irregular shapes. Fig. 10(b) shows a typical EBSD map of the microstructure shown in Fig. 10(a). The corresponding PFs are shown in Fig. 10(c) and show a distinct twinning relationship. The yellow curves in Fig. 10(b) indicate the twin boundary, that is, the Σ3 60° <111> boundary

(with a maximum deviation of 5°). The red dashed lines in Fig. 10(b) and (c) indicate the common {111} twin plane. As seen in Fig. 10(b), the twin boundary trace (yellow curve) is not consistent with the theoretical {111} lattice plane (red dashed line), which indicates the incoherence of the twin boundary.

It should also be noted that there were indeed some small lattice deflections present in the PFs in Fig. 10(c) (indicated by arrows). Fig. 10(d) and (e) show the misorientation measured along the white dotted lines 1 and 2 in Fig. 10(b). The misorientation along line 2 was 57.52°, with a deviation of approximately 2.5° around the <111> axis from a twinning relationship. Furthermore, Fig. 10(f) shows the overall misorientation angle distribution for the microstructure in Fig. 10(b). As seen in the inset EBSD map, the lower right boundary went through a general angular deflection, and this corresponds to the relative frequency peak present in the range from 56°-60°. In the upper region of the EBSD map, a low-angle boundary (~4.23°) is present, and this corresponds to the peak at the left side of Fig. 10(f). The rather low V caused these sophisticated structural and crystallographic changes in the twins during solidification. Also, the solidification at 0.5 μm/s was not yet planar growth because there were several small droplets of Mg-rich liquids that were still within the scope of the cellular interface (Fig. 9(h2) and Fig. 10(a)).

3.3 Stability analysis of the twin boundary during directional solidification

The coherent and incoherent twin boundaries (TBs) are the unique structural morphology owned by twinned dendrite and cell grains, and distinguish them from regular columnar and equiaxed grains. The stability analysis of TBs under various growth conditions is necessary for understanding twin solidification in Al alloys.

Concerning the grain boundary grooves that are present on the S/L interface, Tiller et al. [34] proposed a criterion based on the constitutional undercooling theory to estimate their growth stability. The grain boundary grooves at the interface are maintained and do not

shrink when:

$$\frac{G_S}{V} < \frac{m_L C_0 (k_0 - 1)}{k_0 D_L} \quad (1)$$

where G_S is the thermal gradient in the solid near grain boundary grooves, m_L is the slope of the liquidus, C_0 is the initial solute concentration of the experimental alloy, D_L is the liquid diffusion coefficient, and k_0 is the partition coefficient.

Table 1. Thermophysical properties of the Al-Mg alloy used in the calculation.

Parameter (Unit)	Value	Refs.
Liquid diffusion coefficient, D_L (m^2/s)	1.5×10^{-9}	[35]
Average thermal gradient in the liquid, G (K/cm)	~269	
Liquidus slope, m_L (K/wt.%)	-5.8	
Equilibrium partition coefficient, k_0	0.472	[35]
Liquid thermal conductivity, k_L (W/(m·K))	92.6	[35]
Solid thermal conductivity, k_S (W/(m·K))	130	[35]

This criterion can help explain the stability of TBs in twinned dendrites, which is a typical large-angle grain boundary. Using Eq. (1), the critical V for maintaining TBs during solidification can be expressed as follows:

$$V_T = \frac{k_0 D_L}{m_L (k_0 - 1)} \cdot \frac{G_S}{C_0} \quad (2)$$

For a planar front interface in metals, $k_L G \approx k_S G_S$ where k_L and k_S are the thermal conductivities of the liquid and solid, respectively. Eq. (2) can be written as follows:

$$V_T = \frac{k_L}{k_S} \cdot \frac{k_0 D_L}{m_L (k_0 - 1)} \cdot \frac{G}{C_0} = \frac{k_L}{k_S} \cdot V_c \quad (3)$$

where V_c is the critical growth velocity that leads to a planar interface being established, according to constitutional undercooling theory [27]. Eq. (3) indicates that TBs might still exist at a rather low growth velocity of V_T, which is less than V_c. By using the Mullins-Sekerka linear stability theory [36], we introduce a more accurate threshold velocity for the planar interface instability:

$$V_c^{MS} = \frac{2 k_0 D_L}{(k_S/k_L + 1) m_L (k_0 - 1)} \cdot \frac{G}{C_0} \quad (4)$$

This expression can be substituted into Eq. (3) to give the following:

$$V_T{}^{MS} = \frac{k_L}{k_S} \cdot V_c{}^{MS} = \frac{2k_0 D_L}{(k_S/k_L+1)m_L(k_0-1)} \cdot \frac{k_L G}{k_S C_0} \quad (5)$$

Substituting the parameters of Table 1 into Eq. (5), the modified critical velocity $V_T{}^{MS}$ was calculated to be 0.37 μm/s. In this case, the TBs would not vanish at values of V that were higher than 0.37 μm/s. This can explain why the TBs were maintained in the solidification experiments at 100 μm/s and 10 μm/s, and even at a low V of 0.5 μm/s. It should be noted that the criterion of Eq. (5) does not consider the coherency of TBs and only focuses on the possibility of their presence at the S/L interface under different solidification conditions. Meanwhile, the above discussions are on basis of the linear theory of morphological stability [27, 28, 36], which provide a starting point for theoretical analysis of the evolution of twin structure in Al alloys. For further consideration, a non-linear stability theory [37, 38] can be extended for the treatment of dynamical stability to learn more about the complex and kinetic details of twin solidification, and it may open a new area of study for exploring complex interface patterns (either theoretically or experimentally) in directional solidification of Al alloys.

4. Conclusions

In this work, twin crystal structured Al-10 wt.% Mg alloys were produced via directional solidification over a wide range of values of V. The microstructure and growth characteristics of twinned dendrites were comprehensively studied. At high values of Vs (500, 1000, 1500, and 2000 μm/s), twinned dendritic trunks in the Al-Mg system generally curved along the G direction with relatively large angles and had a strong kinetics growth advantage. During solidification at 3000 μm/s, twinned dendrite structures were more uniform than those at lower constant values of V, and the trunks became more parallel to the G direction. After quenching, the twinned trunks were found to further bend and have a finer size. Additionally, in the mushy zone, small equiaxed dendrites were observed in the narrow liquid phase between twin lamellae, and the subsequent development of these dendrites can impede

twinned dendrite growth. The twinned dendrites lost their growth advantage over equiaxed ones during free solidification after quenching.

Directional solidification experiments with transitive deceleration were designed to obtain twin crystals for the Al-10 wt.% Mg alloy at lower values of V (100, 10, and 0.5 μm/s). Experimental results showed that when the solidification was decreased to less than 3000 μm/s, the twinned dendrite and twinned cellular structures maintained their growth at 100 μm/s and 10 μm/s while simultaneously containing coherent twin boundaries. However, when V was decreased to 0.5 μm/s, there was a coherency loss of the twin boundaries, and twin domains grew independently and formed curvy incoherent boundaries. Linear stability analysis showed that TBs were present at values of V higher than 0.37 μm/s during directional solidification.

Acknowledgments

This work was supported financially by the Basic Science Center Program for Multiphase Evolution in Hypergravity of the National Natural Science Foundation of China (No. 51988101), Natural Science Foundation of China (No. 51974257, No. 91860202), China Postdoctoral Science Foundation (2018M640031), the fund of the State Key Laboratory of Solidification Processing (Northwestern Polytechnical University) (SKLSP202008, 2019-TS-01), “111” project (DB18015), and Beijing Outstanding Young Scientists Projects BJJWZYJH01201910005018.

References

[1] W. Kurz, D.J. Fisher, R. Trivedi, Progress in modelling solidification microstructures in metals and alloys: dendrites and cells from 1700 to 2000, International Materials Reviews 64(6) (2019) 311-354.
[2] R. Trivedi, W. Kurz, Dendritic growth, International Materials Reviews 39(2) (1994) 49-74.
[3] L. Wang, J.J. Hoyt, N. Wang, N. Provatas, C.W. Sinclair, Controlling solid-liquid interfacial energy anisotropy through the isotropic liquid, Nature communications 11(1) (2020) 1-7.
[4] J. Zhang, B. Song, Q. Wei, D. Bourell, Y. Shi, A review of selective laser melting of aluminum alloys: Processing, microstructure, property and developing trends, Journal of Materials Science & Technology 35(2) (2019) 270-284.
[5] M. Rappaz, P. Jarry, G. Kurtuldu, J. Zollinger, Solidification of metallic alloys: Does the structure of the

liquid matter, Metall. Mater. Trans. A 51A (2020) 2020-2651.
[6] T. Haxhimali, A. Karma, F. Gonzales, M. Rappaz, Orientation selection in dendritic evolution, Nature materials 5(8) (2006) 660.
[7] M.A. Salgado-Ordorica, M. Rappaz, Twinned dendrite growth in binary aluminum alloys, Acta Materialia 56(19) (2008) 5708-5718.
[8] X. Li, Q. Li, Z. Ren, Y. Fautrelle, X. Lu, A. Gagnoud, Y. Zhang, C. Esling, H. Wang, Y. Dai, Investigation on the formation mechanism of irregular dendrite during directional solidification of Al–Cu alloys under a high magnetic field, Journal of Alloys and Compounds 581 (2013) 769-775.
[9] L. Yang, S. Li, X. Chang, H. Zhong, H. Fu, Twinned dendrite growth during Bridgman solidification, Acta Materialia 97 (2015) 269-281.
[10] S. Henry, P. Jarry, M. Rappaz, < 110 > dendrite growth in aluminum feathery grains, Metallurgical and Materials Transactions a-Physical Metallurgy and Materials Science 29A(11) (1998) 2807-2817.
[11] S. Henry, G.U. Gruen, M. Rappaz, Influence of convection on feathery grain formation in aluminum alloys, Metallurgical and Materials Transactions a-Physical Metallurgy and Materials Science 35A(8) (2004) 2495-2501.
[12] A.N. Turchin, M. Zuijderwijk, J. Pool, D.G. Eskin, L. Katgerman, Feathery grain growth during solidification under forced flow conditions, Acta Materialia 55(11) (2007) 3795-3801.
[13] G. Kurtuldu, P. Jarry, M. Rappaz, Influence of Cr on the nucleation of primary Al and formation of twinned dendrites in Al-Zn-Cr alloys: Can icosahedral solid clusters play a role?, Acta Materialia 61(19) (2013) 7098-7108.
[14] G. Kurtuldu, Influence of Trace Elements on the Nucleation and Solidification Morphologies of Fcc Alloys and Relationship with Icosahedral Quasicrystal Formation, Ecole Polytechnique Fe´de´rale de Lausanne, 2014.
[15] M.A. Salgado-Ordorica, J. Valloton, M. Rappaz, Study of twinned dendrite growth stability, Scripta Materialia 61(4) (2009) 367-370.
[16] L. Yang, S. Li, J. Guo, K. Fan, Y. Li, H. Zhong, H. Fu, Pattern selection of twinned growth in aluminum alloys during Bridgman solidification, Journal of Alloys & Compounds 741 (2018) 131-140.
[17] M.A. Salgado Ordorica, Characterization and modeling of twinned dendrite growth, Ecole Polytechnique Fe´de´rale de Lausanne, 2009.
[18] E.H. Sunseri, Dendrite orientation in aluminum magnesium alloys, (2009).
[19] H. Zheng, R. Chen, G. Qin, X. Li, Y. Su, H. Ding, J. Guo, H. Fu, Microstructure evolution, Cu segregation and tensile properties of CoCrFeNiCu high entropy alloy during directional solidification, Journal of Materials Science & Technology 38 (2020) 19-27.
[20] Y. Wang, S. Li, Z. Liu, H. Zhong, L. Xu, H. Xing, Probing the degenerate pattern growth of {100}<011> orientation in a directionally solidified Al-4.5 wt% Cu alloy, Journal of Materials Science & Technology 35(7) (2019) 1309-1314.
[21] S. Shuai, X. Lin, Y. Dong, L. Hou, H. Liao, J. Wang, Z. Ren, Three dimensional dendritic morphology and orientation transition induced by high static magnetic field in directionally solidified Al-10 wt.%Zn alloy, Journal of Materials Science & Technology 35(8) (2019) 1587-1592.
[22] C. Cui, C. Wang, P. Wang, W. Liu, Y. Lai, L. Deng, H. Su, Microstructure and fracture toughness of the Bridgman directionally solidified Fe-Al-Ta eutectic at different solidification rates, Journal of Materials Science & Technology 42 (2020) 63-74.
[23] L.F. Mondolfo, Aluminum alloys: structure and properties, Elsevier2013.
[24] D.G. Eskin, Physical metallurgy of direct chill casting of aluminum alloys, CRC press, New York, 2008.
[25] Q. Luo, Y. Guo, B. Liu, Y. Feng, J. Zhang, Q. Li, K. Chou, Thermodynamics and kinetics of phase transformation in rare earth–magnesium alloys: a critical review, Journal of Materials Science & Technology 44 (2020) 171-190.
[26] D. Zhang, Z. Zhang, Y. Pan, Y. Jiang, L. Zhuang, J. Zhang, X. Zhang, Current-driving intergranular corrosion performance regeneration below the precipitates solvus temperature in Al–Mg alloy, Journal of Materials Science & Technology 53 (2020) 132-139.
[27] W. Kurz, D.J. Fisher, Fundamentals of Solidification, Trans Tech Publications Limited1998.
[28] J.A. Dantzig, M. Rappaz, Solidification: 2nd Edition - Revised & Expanded, EPFL Press2016.
[29] L. Yang, S. Li, Y. Li, K. Fan, H. Zhong, Study of growth advantage of twinned dendrites in aluminum alloys during Bridgman solidification, Journal of Materials Research 34(2) (2019) 240-250.
[30] A.N. Turchin, D.G. Eskin, L. Katgerman, Solidification under forced-flow conditions in a shallow cavity, Metallurgical and Materials Transactions a-Physical Metallurgy and Materials Science 38A(6) (2007) 1317-1329.
[31] X. Lin, W. Huang, J. Feng, T. Li, Y. Zhou, History-dependent selection of primary cellular/dendritic spacing during unidirectional solidification in aluminum alloys, Acta Materialia 47(11) (1999) 3271-3280.
[32] J. Hötzer, P. Steinmetz, A. Dennstedt, A. Genau, M. Kellner, I. Sargin, B. Nestler, Influence of growth velocity variations on the pattern formation during the directional solidification of ternary eutectic Al-Ag-Cu,

Acta Materialia 136 (2017) 335-346.
[33] G. Kurtuldu, P. Jarry, M. Rappaz, Influence of minor Cr-additions to the growth of columnar dendrites in Al-Zn alloys: Influence of Icosahedral Short Range Order in the liquid, Metallurgical and Materials Transactions A 51(1) (2020) 279-288.
[34] W.A. Tiller, The Science of Crystallization: Macroscopic Phenomena and Defect Generation, Cambridge University Press, Cambridge, 1991.
[35] C.J. Vreeman, F.P. Incropera, The effect of free-floating dendrites and convection on macrosegregation in direct chill cast aluminum alloys Part II: predictions for Al-Cu and Al-Mg alloys, International Journal of Heat and Mass Transfer 43(5) (2000) 687-704.
[36] W.W. Mullins, R. Sekerka, Stability of a planar interface during solidification of a dilute binary alloy, Journal of applied physics 35(2) (1964) 444-451.
[37] M.E. Glicksman, Principles of Solidification: An Introduction to Modern Casting and Crystal Growth Concepts, Springer New York2010.
[38] C. Godrèche, B.-R.S. School, C.G. Che, Solids Far from Equilibrium, Cambridge University Press1992.